PNAS
www.pnas.org

Supplementary Information for

A polyyne toxin produced by an antagonistic bacterium blinds and lyses a Chlamydomonad alga

Vivien Hotter[1], David Zopf[2,3], Hak Joong Kim[4], Anja Silge[2,3], Michael Schmitt[2], Prasad Aiyar[1], Johanna Fleck[2,3], Christian Matthäus[3], Julian Hniopek[2,3], Qing Yan[7], Joyce Loper[8], Severin Sasso[1,6], Christian Hertweck[4,5]*, Jürgen Popp[2,3]*, Maria Mittag[1]*

[1]Matthias Schleiden Institute of Genetics, Bioinformatics and Molecular Botany, Friedrich Schiller University Jena, 07743 Jena, Germany

[2] Institute of Physical Chemistry & Abbe Center of Photonics, Friedrich Schiller University Jena, 07743 Jena, Germany

[3] Department of Spectroscopy & Imaging, Leibniz Institute of Photonic Technology, Member of the Leibniz Research Alliance - Leibniz Health Technologies, 07745 Jena, Germany

[4]Leibniz Institute for Natural Product Research and Infection Biology (HKI) Beutenbergstr. 11a, 07745 Jena, Germany

[5]Faculty of Biological Sciences, Friedrich Schiller University Jena, 07743 Jena, Germany

[6]Institute of Biology, Plant Physiology, Leipzig University, 04103 Leipzig, Germany

[7]Department of Plant Sciences and Plant Pathology, Montana State University, Bozeman, MT USA

[8]Department of Botany and Plant Pathology, Oregon State University, Corvallis, OR, USA

*Corresponding authors:

Christian Hertweck, **Email:** christian.hertweck@leibniz-hki.de

Jürgen Popp, **Email:** juergen.popp@leibniz-ipht.de

Maria Mittag, **Email:** M.Mittag@uni-jena.de

This PDF file includes:

Supplementary Materials and Methods

Figures S1 to S16

Tables S1 to S3

SI Note

SI References

Creation of a desaturase mutant (Δ*pgnE*)

P. protegens Pf-5 (thereafter abbreviated as *P. protegens*) was cultivated on LB agar at 30 °C for 2 days and inoculated into Luria-Bertani (LB) medium for further incubation for 1 day. The bacterial cells were collected by centrifugation (5,000 rpm, 5 min). Genomic DNA of *P. protegens* was acquired by using a MasterPure™ complete DNA purification kit (Lucigen, Madison). The *pgnE* gene in the putative protegencin biosynthetic gene cluster was PCR amplified from the genomic DNA of *P. protegens* with specific primers (Table S3) and ligated with the apramycin resistance gene. The combined gene fragment was inserted into pJET1.2/Blunt vector. *Escherichia coli* TOP10 competent cells were transformed with the corresponding vector using electroporation (2,500 V). The transformed cells were incubated on LB agar and medium with apramycin and ampicillin at 37 °C for 1 day. The vector containing the combined gene fragment was purified by using a Monarch® Plasmid Miniprep Kit (New England BioLabs, Frankfurt am Main). The transformation of *P. protegens* with the corresponding vector was conducted by electroporation at 2,500 V, and the transformed cells were incubated on LB agar containing apramycin and ampicillin at 30 °C. The colony containing the corresponding mutation was inoculated into LB medium with apramycin and ampicillin and further incubated at 30 °C until OD_{600} value became 4–5. The bacterial cells were collected by centrifugation (5,000 rpm, 5 min) and washed with Tris-Acetate-Phosphate (TAP) medium twice. The collected cells were incubated in TAP medium with ampicillin and apramycin at 30 °C for 1 day for further analytic procedures.

General analytic procedures

Analytic high-performance liquid chromatography (HPLC) measurements were performed on a Shimadzu Prominence HPLC system consisting of an autosampler, high-pressure pumps, column oven and PDA using a Macherey-Nagel C18 reverse phase column (Nucleosil 100, 5 µm, 125 × 4.6 mm, flow rate 1 mL min^{-1}). HPLC grade acetonitrile and deionized water with 0.1% trifluoroacetic acid (TFA) were used as mobile phase for HPLC. The gradient elution for HPLC operation was from 0.5/99.5 of CH_3CN/H_2O with 0.1% (v/v) TFA to 100/0 for 5–35 min. Preparative HPLC measurement were performed on a Gilson Abimed equipped with Binary Pump 321 and 156 UV/Vis detector (eluents: water with 0.1% (v/v) TFA and acetonitrile) using a Macherey-Nagel C18 reverse phase column (Nucleosil 100, 5 µm, 250 × 10 mm, flow rate 5 mL min^{-1}). Liquid chromatography-mass spectrometry (LC-MS) measurements were performed using a QExactive Orbitrap High Performance Benchtop LC-MS with an electrospray ion source and an Accela HPLC system (Thermo Fisher Scientific, Bremen, Germany). For MS/MS measurements, an Exactive Orbitrap mass spectrometer with an electrospray ion source (Thermo Fisher

Scientific, Bremen, Germany) was used. NMR spectra were recorded on Bruker AVANCE III 500 and 600 MHz (equipped with a Bruker Cryo platform) instruments.

Protegencin isolation and CuAAC reaction

P. protegens was cultivated on LB agar at 30 °C for 2 days and inoculated into TAP medium. The bacterial culture was incubated at 30 °C with orbital shaking (150 rpm) for 1 day. The bacterial culture was extracted with ethyl acetate three times. The combined organic layers were reduced under rotary evaporation. The crude extract was purified by putative HPLC and silica gel column (Hex/EtOAc = 1:1) to remove extra fatty acids. The CuAAc reaction procedure was followed as previously reported (1). NMR and MS data of the triazol compound from click reaction with protegencin and benzyl azide are same as reported one (1).

Bright field microscopy of co-cultures

To determine the percentage of algal cells with one and no eyespots or multiple eyespot particles in the different co-cultures, 1 ml cell suspension was taken under sterile conditions after 0, 16, and 24 h of inoculation, respectively, concentrated at 4,500×*g* for 5 min at room temperature, and resuspended in 500 µl TAP. Cells were not fixed. Prior to examination, cells were allowed to settle on the microscope slide for a few minutes at room temperature in the dark. Pictures of at least 100 individual cells per co-culture and time point were taken with an Axiophot (Carl Zeiss, Germany). Each time, an axenic *C. reinhardtii* culture was examined the same way as a control. The percentage of cells with one and no eyespots based on the yellowish color of its carotenoids or multiple eyespot particles was analyzed visually. The experiments were conducted three times independently.

Evans blue assay

For the Evans blue assay, the algal cell density was adjusted to 2×10^6 cells mL^{-1} in the alga's respective culture medium. Subsequently, cells were split in three technical replicates per treatment and each technical replicate treated with 2% (v/v) DMSO and 2% (v/v) protegencin, respectively, for 24 h. In addition, these experiments were performed with treatments of 0.5% DMSO and 0.5% protegencin, respectively. 10 µM mastoparan was used as a positive control for 30 s, as well as ddH_2O, the compound's solvent (2). For the duration of the treatment, the cells were kept shaking in the dark at room temperature. Subsequently, the cells were washed three times with their respective culture medium and finally resuspended in 0.1% (w/v) Evans blue in TAP. After incubation at room temperature for 5 min, the percentage of stained cells was

determined by brightfield microscopy (Axiophot, Carl Zeiss, Germany). At least 500 cells per technical replicate were examined.

Survival assay

To obtain the amount of colony forming units (CFUs) of *C. reinhardtii* and of the *eye3-2* mutant CC-4316 in the presence of protegencin as a means of algal survival rate, the algal cell density was adjusted to 2×10^6 cells mL^{-1} in the respective culture medium. Subsequently, cells were treated with 0.5% (v/v) DMSO and 0.5% (v/v) protegencin, respectively, for either 1 h or 4 h. An untreated control was handled identically. For the duration of the treatment, the cells were kept shaking in the dark at room temperature. Each treatment was serially diluted in the respective culture medium to a final dilution of 1:10,000. 100 µl of each dilution were plated on culture medium agar plates in triplicates and incubated at 23 °C under a 12:12 LD regime white light of an intensity of 50 $\mu mol \cdot m^{-2} \cdot s^{-1}$ for 7 days. The percentage of surviving algae was calculated based on the CFUs visible after 7 days.

In case of *G. pectorale*, no CFUs were determined as the alga needs very long time periods (more than 4 weeks) to form single visible colonies on agar plates. Instead, the alga was treated as described above, but rather than serially diluted and plated, 100 µl of each technical replicate and treatment (0.5% (v/v) DMSO as control and 0.5% (v/v) protegencin) were added to 5 ml fresh liquid culture medium after the 4 h incubation. The untreated control was handled identically. After 5 days of growth under a 12:12 LD regime with white light of an intensity of 50 $\mu mol \cdot m^{-2} \cdot s^{-1}$ and shaking (200 rpm), the percentage of surviving algae was calculated based on the cell count in the cultures.

Marker band regions

Raman intensity maps were calculated by summing over compound specific marker bands. We distinguished four components in the analysis namely starch, typical cell compounds, carotenoid and protegencin. Particularly for starch, the analysis included only sharp prominent bands not overlaid by other Raman band features. The three marker bands for typical cell compounds were associated with lipids and proteins with rather broad Raman bands centered at 1451 cm^{-1}, 1660 cm^{-1} and 2920 cm^{-1}. The used Raman bands and their corresponding integration regions are listed in Table S1.

Segmentation and background correction

Before further analysis of the hyperspectral Raman images, segmentation of the latter in cell and background areas was performed. Furthermore, the previously performed background correction by the SNIP algorithm was supplemented by an additional correction taking the embedding (0.5% agarose) into account. For this purpose, the compound maps of starch, cell, and carotenoid marker bands were normalized on their corresponding maxima and summed up to an intensity map $I_{Cell}(x, y)$ which includes all cell components (Fig. S3A). Afterwards the mean value of the obtained intensity map was computed. The mean value served as threshold and pixel values in $I_{Cell}(x, y)$ below or equal to the mean value were assigned as background pixels whereas pixels in $I_{Cell}(x, y)$ with values greater than the mean were assigned cell pixels. Contiguous pixel areas smaller than 100 pixels in the resulting binary cell/background map were assigned to background pixels. The inset in Fig. S3B shows an exemplary binary image of the scanned area segmented in algae cell area (red) and background area (blue).

Using the background pixels found, a background correction of the Raman pixel spectra associated with the algal cells was performed to minimize the influence of the background signal originating from the 0.5% agarose embedding. For this, all Raman pixel spectra associated with the background were averaged (see blue spectrum in Fig. S3B). This background spectrum was then subtracted from all pixel spectra. Moreover, all single pixel spectra associated with background pixels were then substituted by the newly corrected average background spectrum. Latter was performed to avoid unnecessary fragmentation of the background area by the k-means-cluster-analysis.

The background corrected hyperspectral Raman image served further as the basis for the calculation of the presented Raman intensity maps and were employed for further analysis including k-means cluster analysis, carotenoid detection and the evaluation of the protegencin content in single algae cells.

K-means cluster analysis

A k-means cluster analysis with k = 7 was carried out after the above described background correction (3). The spatial cluster arrangement was visualized in false-color-plots after color-coding each cluster.

Carotenoid detection

To identify carotenoid clusters in single algae cells a fit of a Lorentzian profile $L(\nu; \nu_0, A, \Gamma) = A \cdot \Gamma / [(\nu - \nu_0)^2 + \Gamma^2]$ was applied in each of the three marker band regions associated with carotenoid: 1004±20 cm^{-1}, 1157±20 cm^{-1}, and 1523±20 cm^{-1}. Only pixel spectra where all three fits converged were considered for further analysis. We applied an additional constraint to

the resulting fit amplitudes *A*: the amplitudes of the Lorentzian profile should be greater than the average spectral intensity plus three times the intensity standard deviation in the wavenumber range 10 cm^{-1} above the corresponding carotenoid spectral region. For instance, the amplitude *A* computed by a Lorentzian fit model in the wavenumber region of 1004±20 cm^{-1} must be greater than the average spectral intensity plus the three times intensity standard deviation ranging from 1025 cm^{-1} to 1035 cm^{-1}. Latter constraint was applied to avoid that pixel with spectral noise are assigned falsely as carotenoid pixels. Pixel spectra fits which did not fulfill these requirements were discarded as possible carotenoid pixels. Contiguous pixel areas smaller than 4 pixels in the resulting binary map were discarded as well.

Evaluation of the protegencin content

The metric "Intensity(2160)/Intensity(1451)", defined as the ratio of the integrated spectral intensities of the peak features at 2160 cm^{-1} and 1451 cm^{-1} (see Table S1), served as a measure of the protegencin content. For this purpose, the integrated spectral intensities of the assigned algal cell pixels of the hyperspectral Raman image were averaged and the ratio of the latter was calculated for each investigated algal cell.

Density Functional Theory calculations of protegencin and its Raman spectrum

To confirm the detection of protegencin inside *via* Raman Spectroscopy, Density Functional Theory (DFT) calculations were performed on the *trans*-structure of protegencin. The calculations were performed using Orca (version 4.2) (4, 5). First, a relaxed geometry optimization was performed using the hybrid gradient corrected functional B3LYP (6, 7), and polarized triple-ζ basis-set def2-TVZP combined with empirical dispersion correction using the Becke-Johnson damping scheme (8-10). To speed up the calculation resolution of identity approximation for the coulomb integrals with the auxiliary basis set def2/J was used (11, 12).

To confirm that the calculated spectrum represents a minimum in the 3N-6 dimensional potential energy hyperplane and to calculate the Raman spectrum, a subsequent numerical frequency and polarizability calculation was performed using the same functional and basis set, which allows for the calculation of Raman activities.

The calculated Raman activities were converted to Raman intensities by employing the following equation (13):

$$R_i = \frac{(2\pi)^4}{45} \cdot (\nu_0 - \nu_i)^4 \cdot \frac{h}{8\pi^2 c \nu_i \left[1 - e^{-\frac{hc\nu_i}{kT}}\right]} \cdot S_i(1)$$

Herein $R_i, S_i, \nu_i, \nu_0, h, c, T, k$ represent the Raman intensity, Raman activity, vibrational frequency of the ith band, frequency of the incident laser light (in this experiment $3.819 \cdot 10^{14}$ Hz or 785 nm), Planck's constant, the speed of light in vacuum, the temperature (in this case 298K / 25 °C), and Boltzmann's constant. To account for the missing description of anharmonicity and electron correlation in the calculated frequencies, an empirical correction factor of 0.965 was employed (14). To visualize the spectra the calculated line spectrum was broadened using a Lorentzian function with a full-width-at-half-maximum of 18 cm^{-1}.

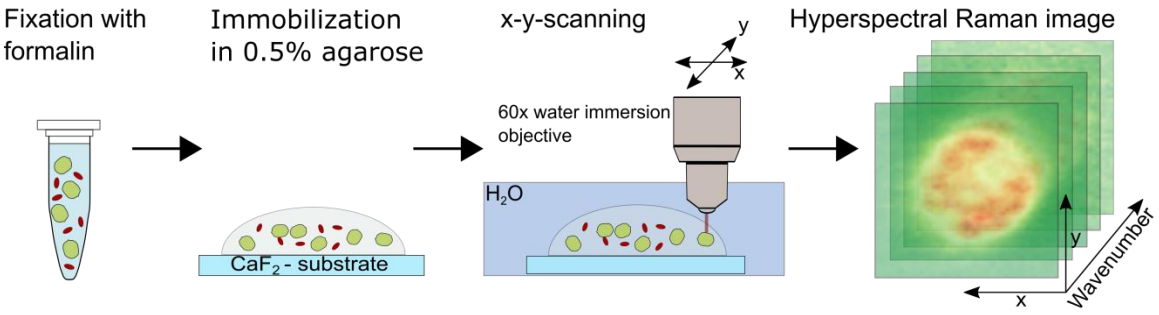

Fig. S1. Schematic of the sample preparation for Raman microspectroscopy and measurement principle. After the fixation of the algal cells in 4% v/v formalin, the algal cells were immobilized in 0.5% agarose in TAP medium and transferred on a CaF_2-platelet. Raman measurements were conducted in aqueous environment and a hyperspectral Raman image was generated by point-wise integration of a 15 µm × 15 µm large scanning grid.

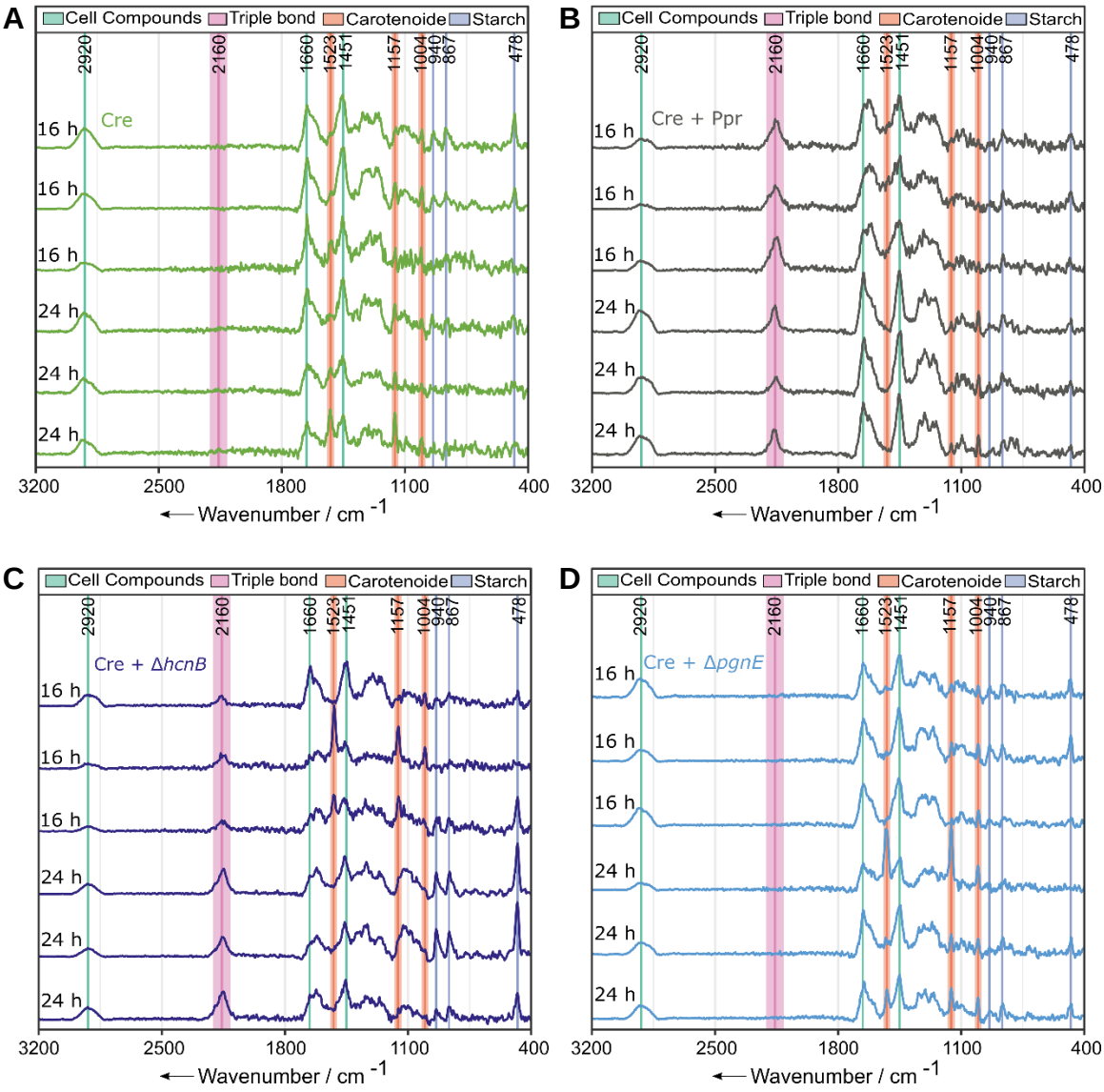

Fig. S2. Representative Raman spectra of *C. reinhardtii* cells grown in mono-culture (Cre, A) or in co-cultures of *C. reinhardtii* cells with *P. protegens* (Ppr) wild type (B) or its mutants Δ*hcnB* (C) or Δ*pgnE* (D) after 16 h and 24 h, respectively. For each timepoint and for each culture condition, three representative spectra are shown.

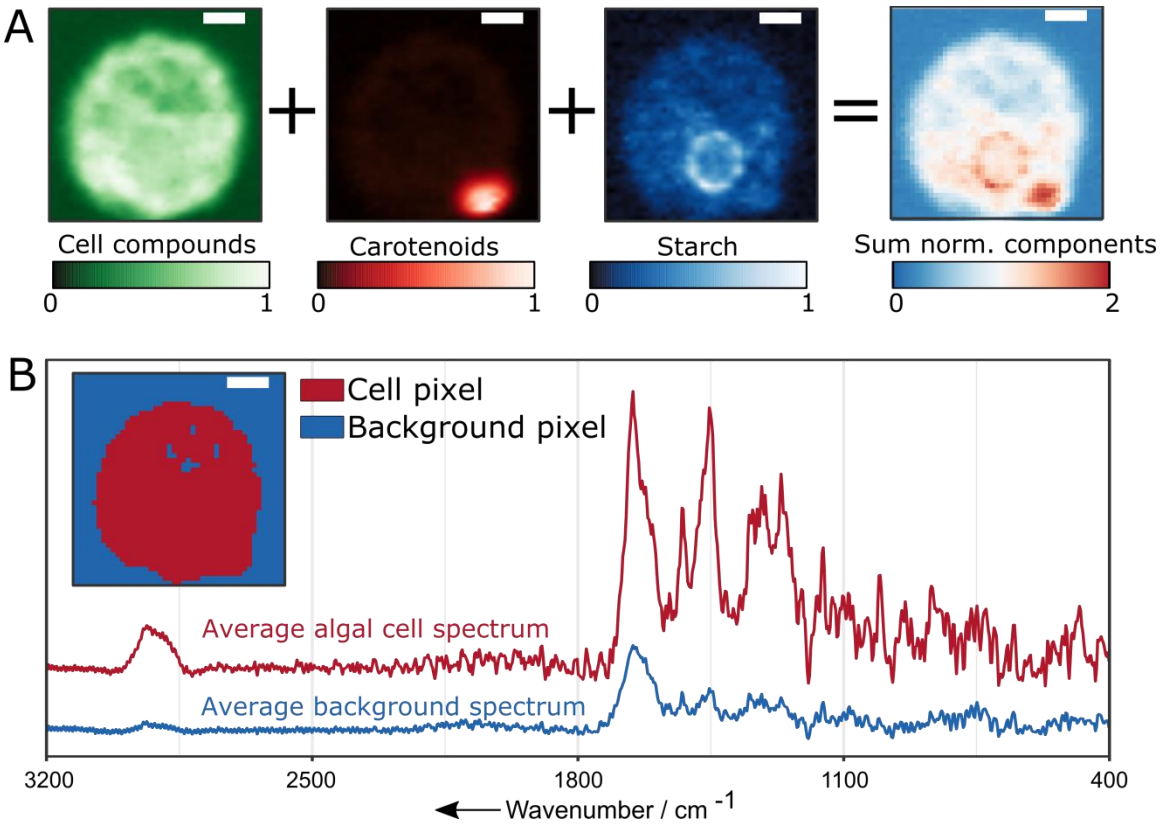

Fig. S3. Raman microspectroscopic image segmentation and calculation of background spectrum. A) Schematic representation of the workflow to compute an overall intensity map for all cell components by summing the normalized Raman intensity maps of the overall cell compounds, carotenoids, and starch. B) Average Raman algal cell (red) and background spectrum (blue) derived from the spectra corresponding to cell and background pixels (see inset for segmentation). Scale bars: 3 µm. For details see Supplementary Information, section segmentation and background correction.

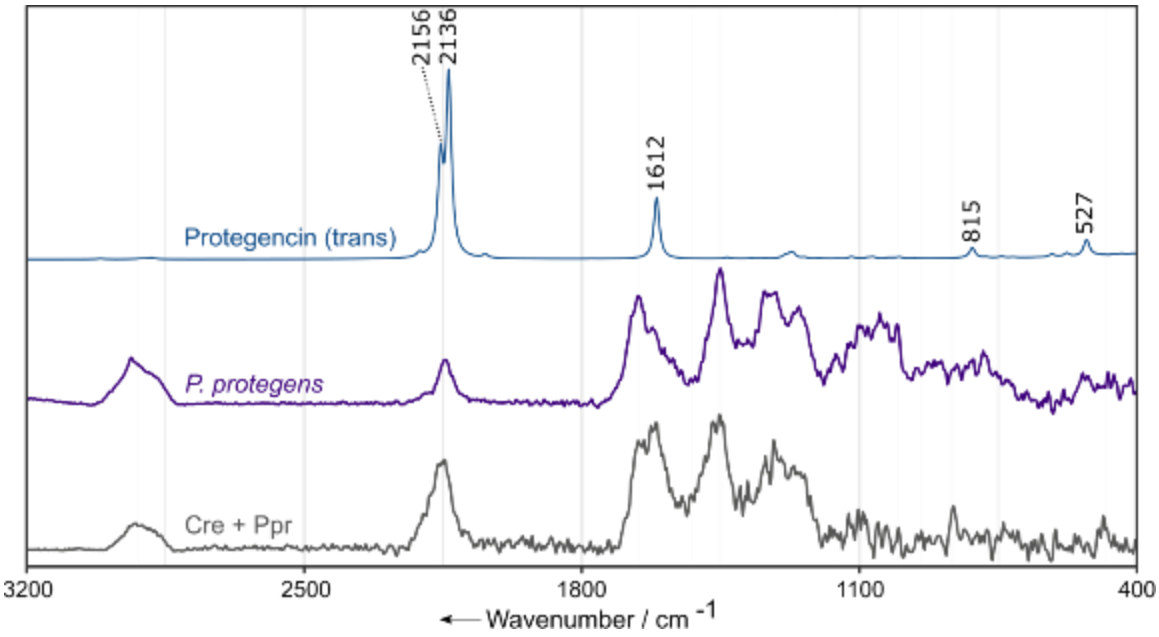

Fig. S4. Comparison of experimental and simulated Raman spectra. The grey spectrum depicts the average Raman spectrum of an exemplary *C. reinhardtii* cell co-cultivated with *P. protegens* after 16 h incubation time (Cre + Ppr). The purple graph depicts the Raman spectrum of axenic *P. protegens* bacteria after 24 h growth in TAP medium. The theoretical Raman spectrum shown in blue depicts the calculated Raman spectrum of protegencin in *trans*-form.

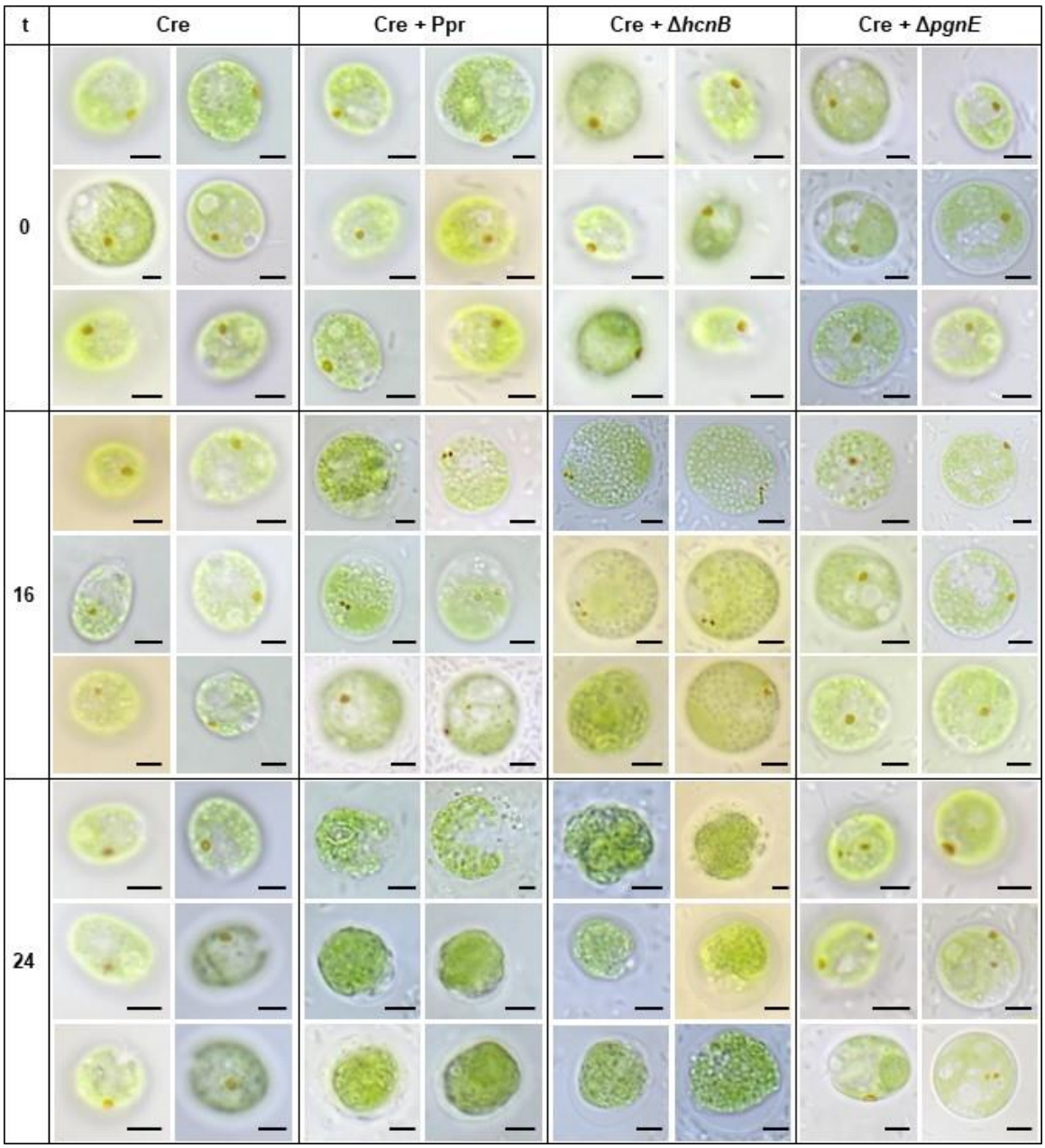

Fig. S5. Representative brightfield microscopy pictures of *C. reinhardtii* cells from mono-cultures (Cre) as well as in co-culture with *P. protegens* (Cre + Ppr) or its mutants (Cre + Δ*hcnB* or Cre + Δ*pgnE*) after 0, 16 and 24 h of incubation. Scale bars: 3 µm.

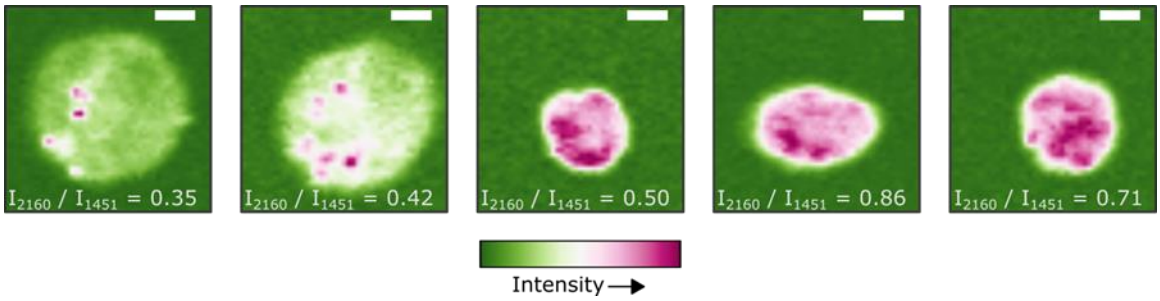

Fig. S6. Distribution of the triple bond substance in five exemplary cells of *C. reinhardtii* after co-culture with *P. protegens* for at least 16 h. Note: The shown Raman intensities depict the integrated intensities solely after the SNIP background correction to demonstrate that the embedding 0.5% agarose gel gives no contribution to the triple bond peak feature. The ratios I_{2160}/I_{1451} are the average Raman intensities associated with the triple bond compound (2,160 cm^{-1}) vs. a dominant band representing *C. reinhardtii* cellular material (C-H deformation mode at 1,451 cm^{-1}) within the detected cell area (see "Evaluation of the protegencin content" for computational details in SI methods). The corresponding cell ratios for all investigated cells with varying co-culture conditions are visualized and summarized as box plots in Fig. 2B; Fig. 3G and Fig. S7B. Scale bars: 3 µm.

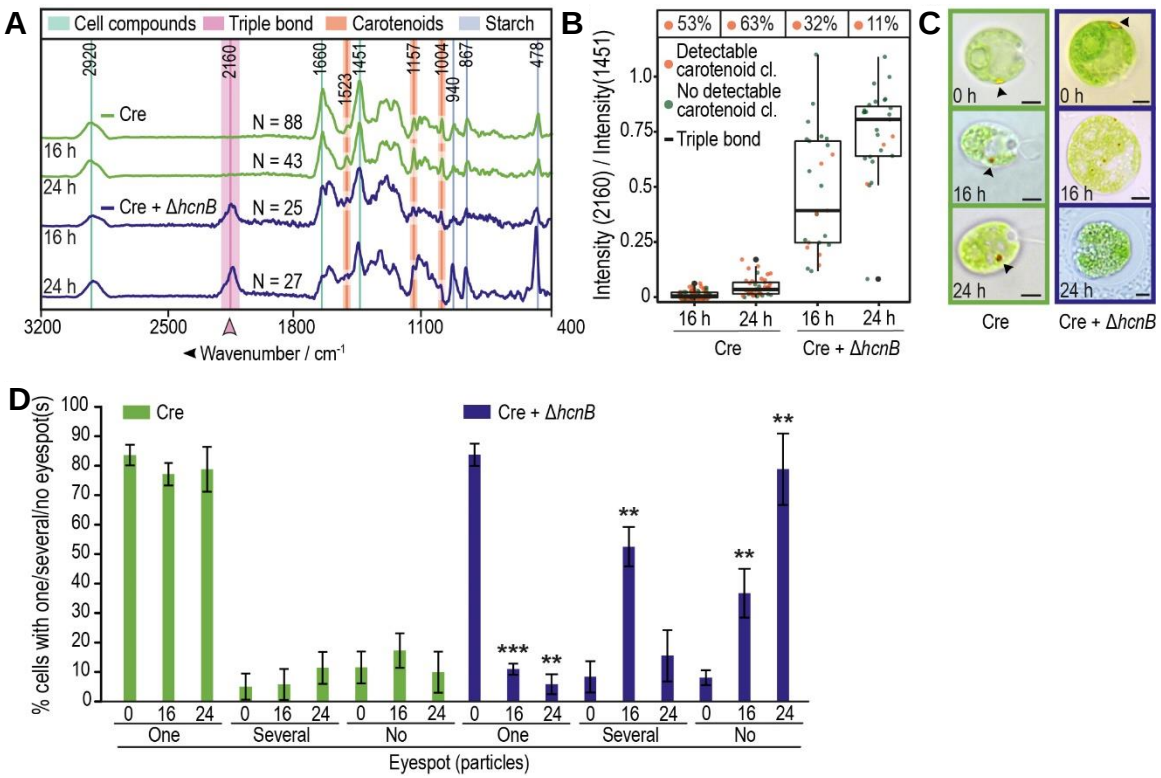

Fig. S7. Disappearance of eyespot carotenoids persists in the *ΔhcnB* cyanide mutant. A, D) Average Raman spectra of *C. reinhardtii* show a peak at 2160 cm^{-1} and reduction of detectable carotenoid peaks over time when co-cultured with *P. protegens* mutant Δ*hcnB* (A, Cre + Δ*hcnB*) compared to axenic *C. reinhardtii* (A). Cultures were grown for 16 or 24 h in TAP. Spectra of algal cells were generated by averaging over all pixels for the relevant Raman spectral class within the cell body. N = total number of analyzed cells. All data were obtained from at least three independent experiments. B) Summary of Raman spectroscopic measurements from A show the presence of the triple bond compound TC (box plot) and a reduction of carotenoid clusters in co-cultures (Cre + Δ*hcnB*). The data points plotted are for the ratio of average Raman intensities associated with the TC (2,160 cm^{-1}) vs. a dominant band representing *C. reinhardtii* cellular material (C-H deformation mode at 1,451 cm^{-1}). Each point represents a measurement of a single alga; box plots indicate quartiles; % values above each box summarize the fraction of cells with detected carotenoid cluster(s). C) Representative brightfield microscopic images of axenic *C. reinhardtii* (green) and in co-culture (C, Cre + Δ*hcnB*, blue) after 0, 16, or 24 h show the disappearance of eyespots as visualized by their carotenoids (see arrowhead) over time in the presence of bacteria. Scale bars: 3 µm. Further cells are shown in Fig. S5. D) Fraction of algal cells (from A–C) with visible eyespots as determined by brightfield microscopy. After 16 h in co-culture, the eyespot is mostly disintegrated, and undetectable based on its color after 24 h, whereas most cells in the axenic culture maintain one eyespot. Asterisks indicate significant

differences as calculated by the Kruskal-Wallis test with Dunn's post-hoc test (**, $P < 0.01$; and ***, $P < 0.001$) in co-culture compared to axenic *C. reinhardtii* at the same time point. Error bars indicate standard deviations with $N \geq 300$ cells per time point and culture.

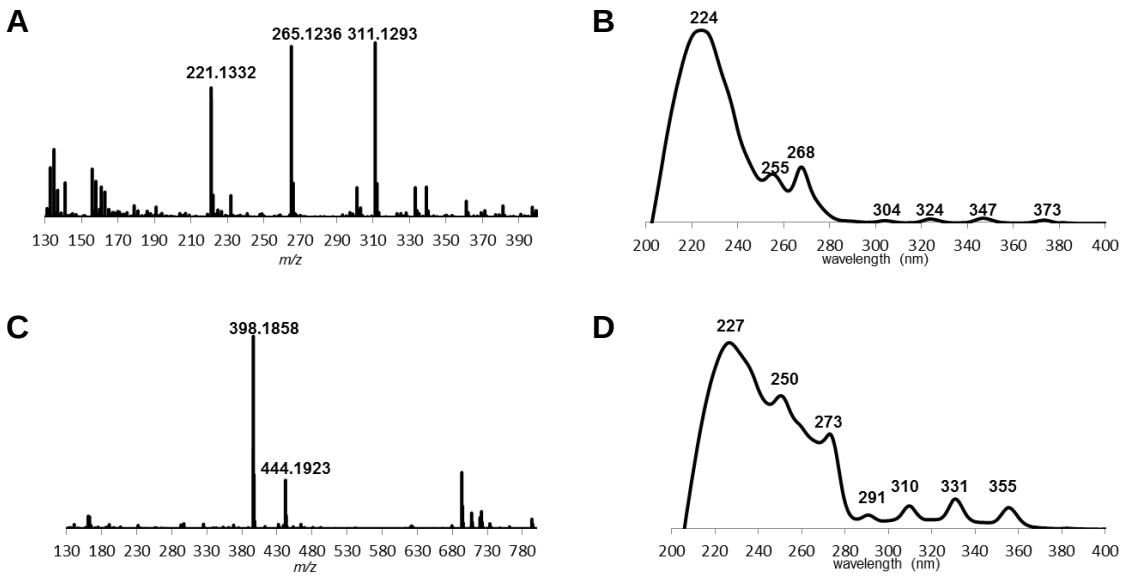

Fig. S8. HRMS and UV spectra of protegencin (A and B) ($C_{18}H_{18}O_2$ [M-H]$^-$ calc. 265.1234, obs. 265.1236) and product of its click reaction with benzyl azide (C and D) ($C_{25}H_{25}N_3O_2$ [M-H]$^-$ calc. 398.1874, obs. 398.1858). Experiments were repeated at least three times.

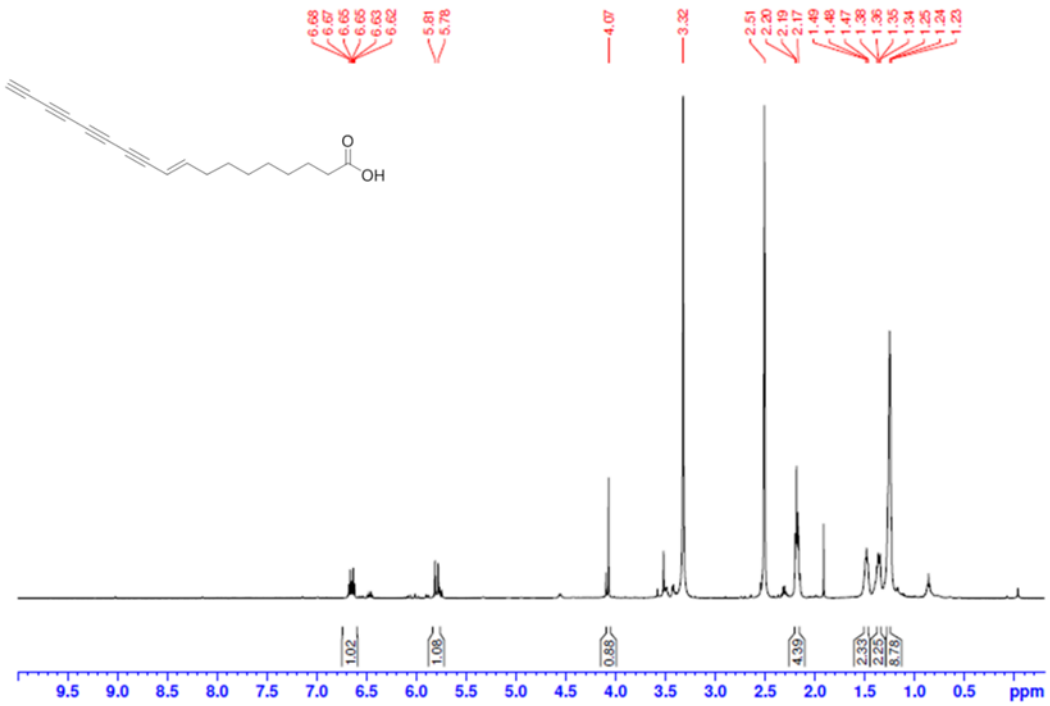

306

307 **Fig. S9**. ^{1}H NMR spectrum of protegencin. Experiments were repeated at least three times.

308

309

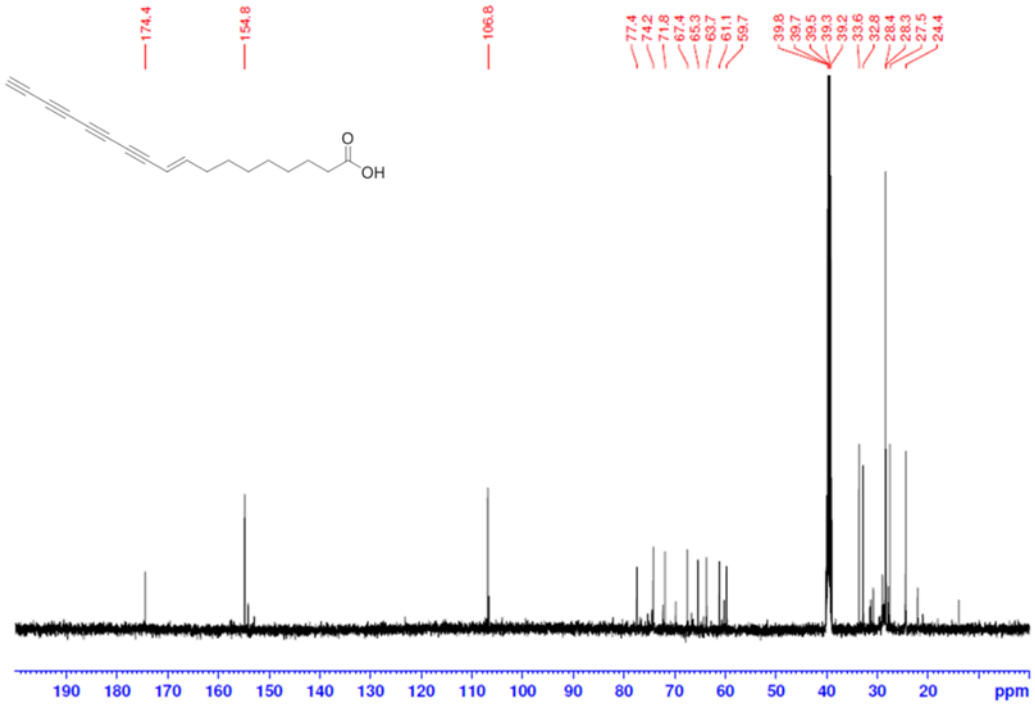

Fig. S10. ^{13}C NMR spectrum of protegencin. Experiments were repeated at least three times.

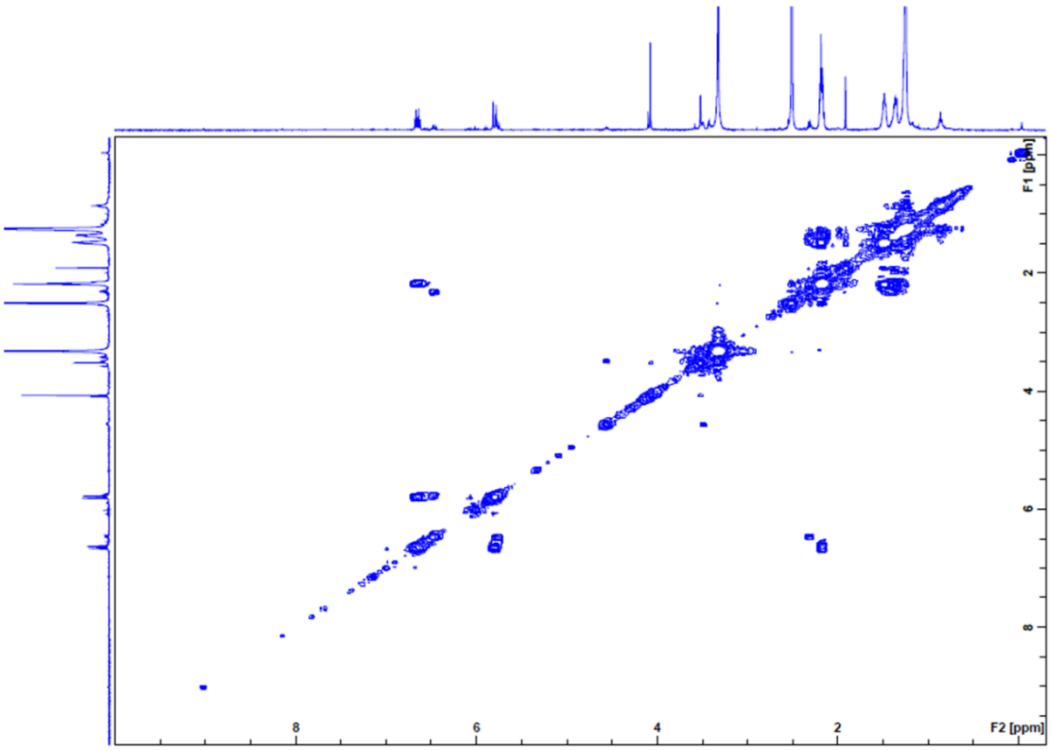

Fig. S11. H,H-COSY NMR spectrum of protegencin. Experiments were repeated at least three times.

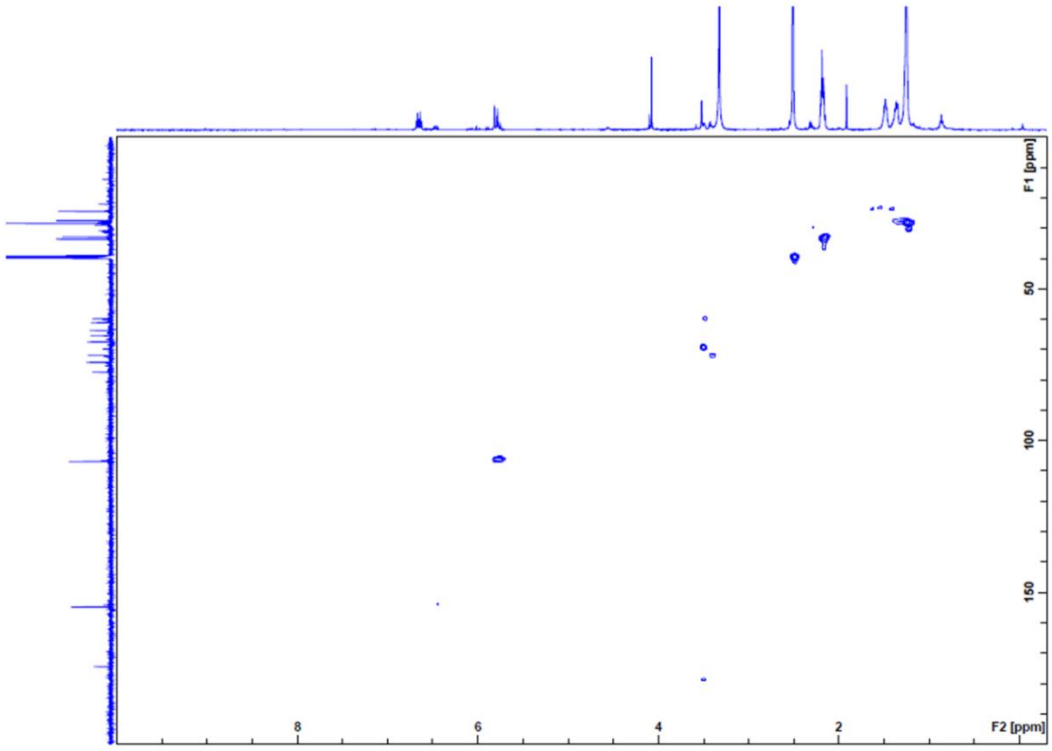

Fig. S12. HSQC NMR spectrum of protegencin. Experiments were repeated at least three times.

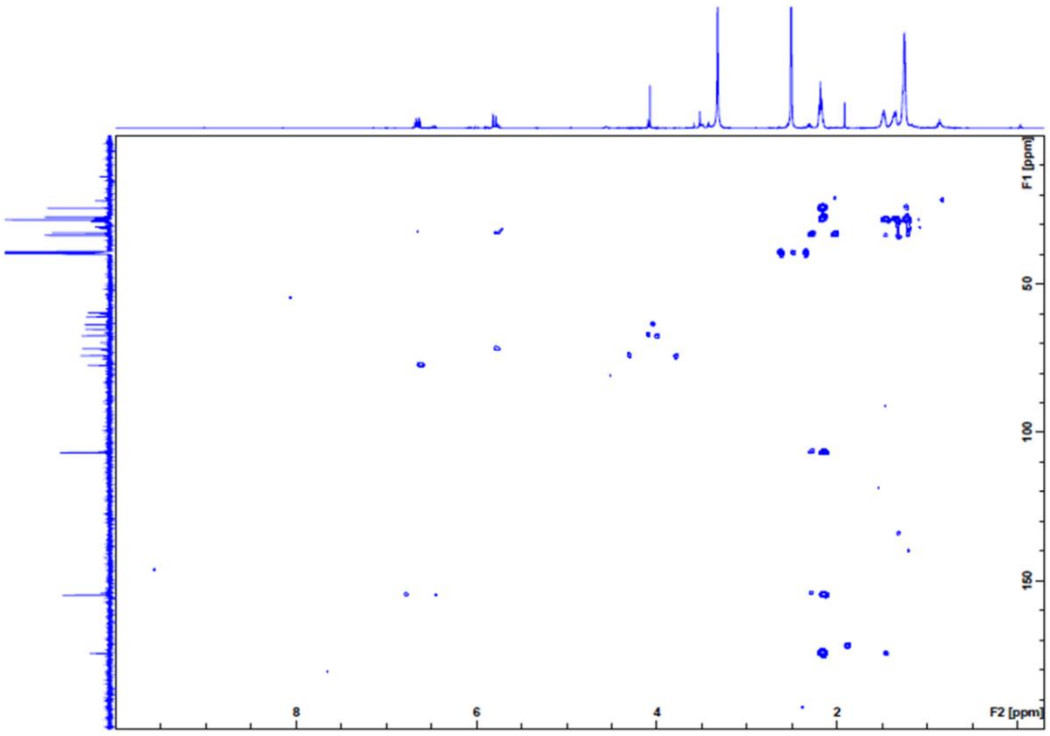

Fig. S13. HMBC NMR spectrum of protegencin. Experiments were repeated at least three times.

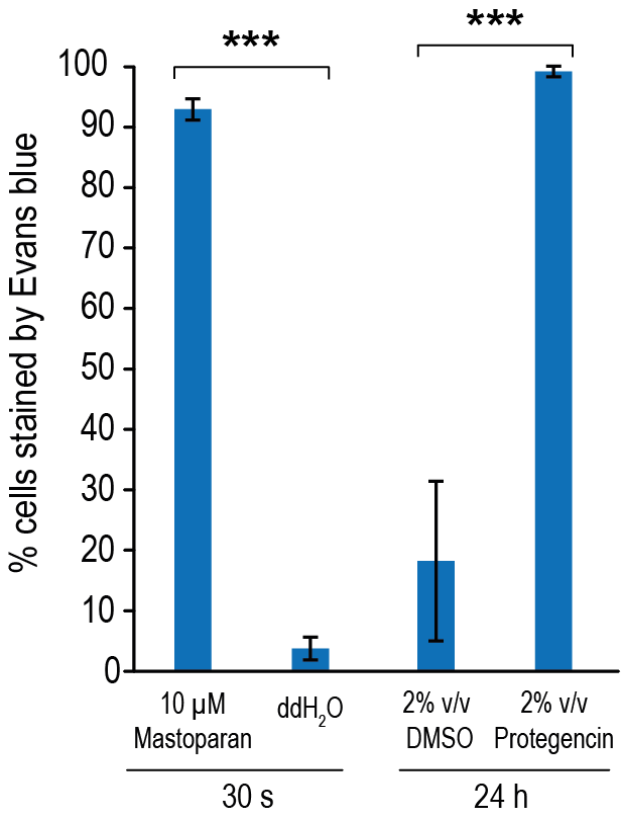

Fig. S14. Evans blue staining of *C. reinhardtii* wild-type strain CC-3348 with 10 µM mastoparan and 2% (v/v) protegencin (equivalent to 10.4 µM). Control treatments with ddH_2O (solvent for mastoparan) (2) and 2% v/v DMSO (solvent for protegencin). Experiments were repeated at least three times independently with three technical replicates each. N ≥ 500 cells per technical replicate. Error bars indicate standard deviations and asterisks indicate significant differences, calculated by Student's t-test (***, $P < 0.001$).

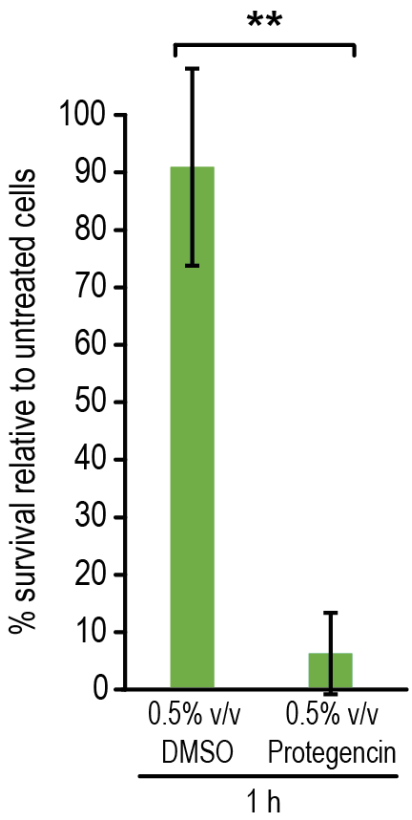

Fig. S15. Survival assay of *C. reinhardtii* wild-type strain CC-3348 after 1 h of incubation with 0.5% v/v protegencin and DMSO (solvent for protegencin), respectively. Experiments were repeated at least three times independently with three technical replicates each. Error bars indicate standard deviations and asterisks indicate significant differences, calculated by Student's t-test (**, $P < 0.01$).

A

Light source

B

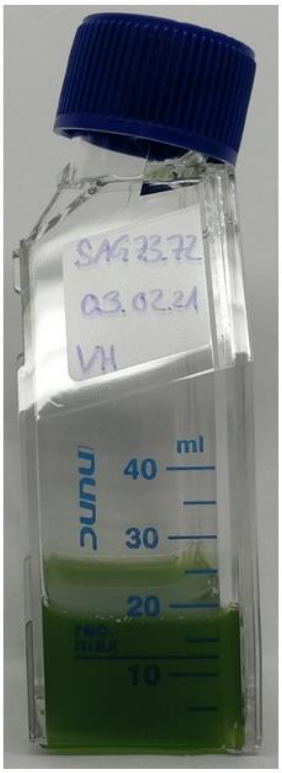

348
349
350
351

C

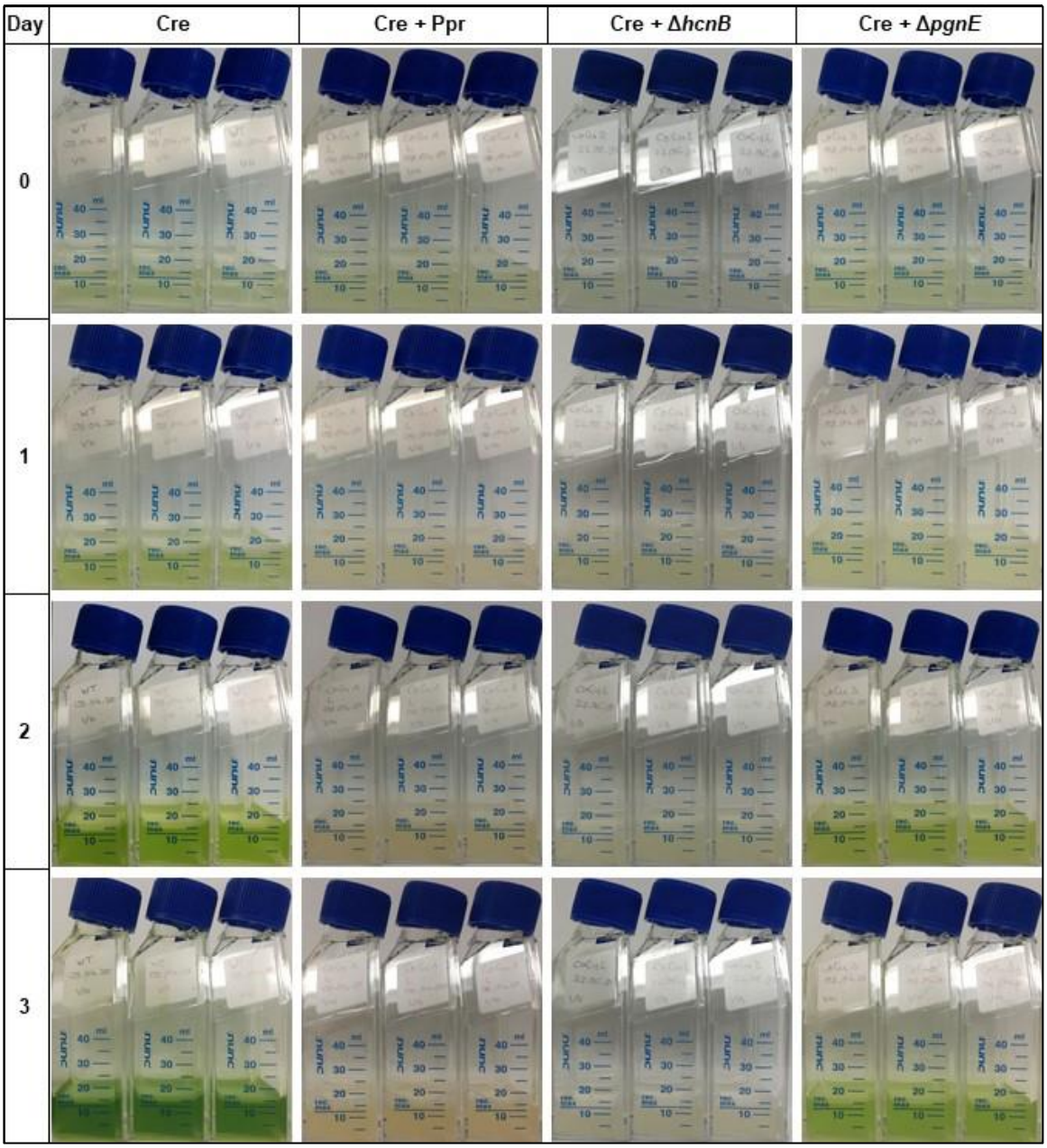

C - continued -

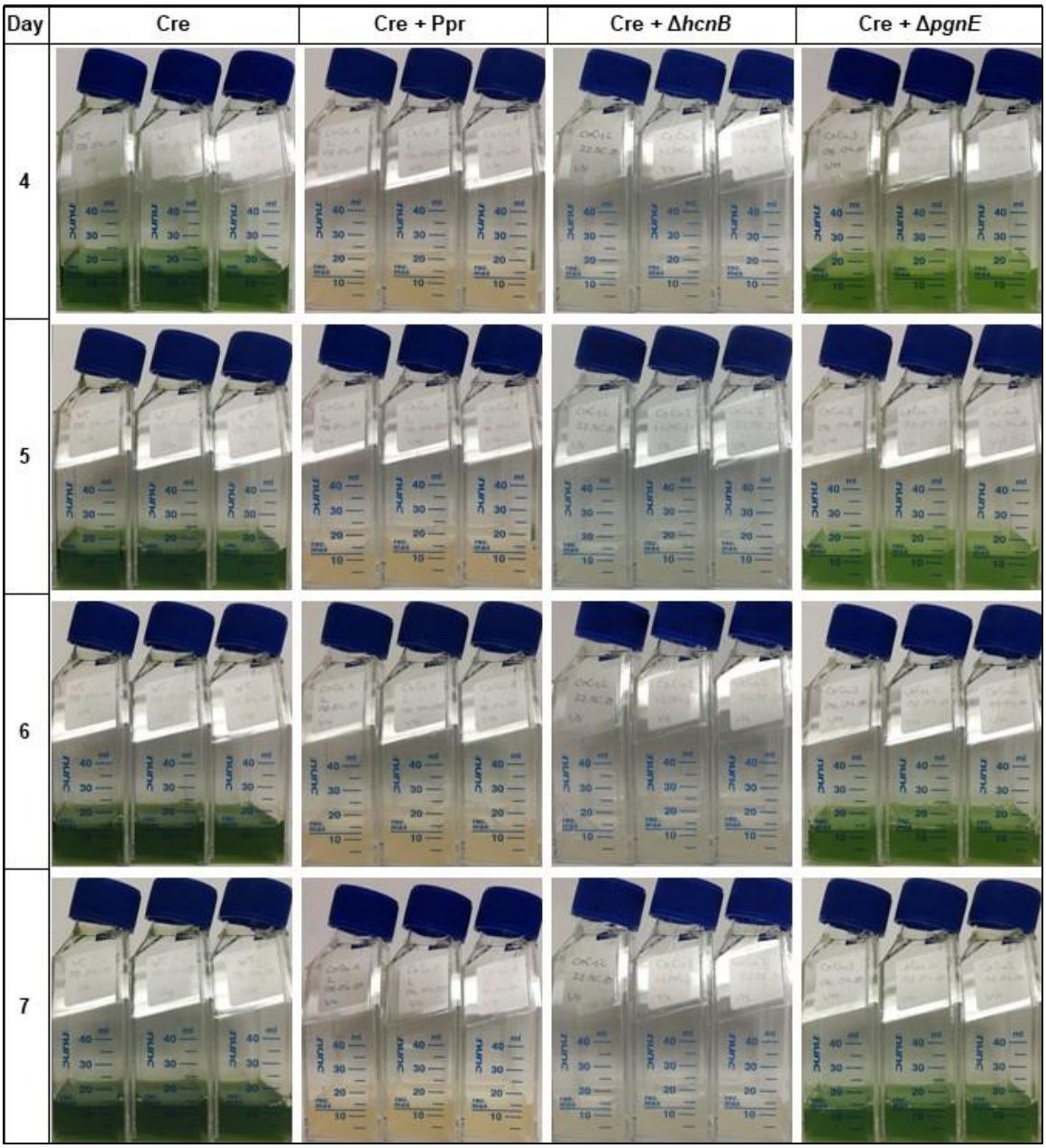

Fig. S16. Mono- and co-cultures of *C. reinhardtii* (Cre) with *P. protegens* (Cre + Ppr) or its mutants (Cre + Δ*hcnB* or Cre + Δ*pgnE*). A) The used cell culture flask for algal growth (NUNC™ EasYFlask™, ThermoFisher Scientific, catalogue number 156367) is shown along with the position of the light source from above. Note that the flasks have a filter membrane in the cap to enable gas exchange. B) For daily photo-documentation, the flasks were put upright. C) Full flasks are shown as seen in a cropped version (only lower parts) in Fig. 4C.

Table S1. Assignment of the Raman bands of the components of interest with their corresponding integration regions.

Wavenumber / cm^{-1}	Integration range / cm^{-1}	Assignment	Reference
478	±20	**Starch**; C–C–C deformation and C–O stretching	(15)
867	±20	**Starch**; C–C–H and C–O–C deformations	(15)
940	±20	**Starch**; C–O–C and C–O–H deformations, C–O stretching	(15)
1004	±20	**Carotenoid**; C–CH_3 rocking	(16)
1157	±20	**Carotenoid**; C–C stretching	(16)
1451	±30	**Cell**; Lipids/proteins: CH_2 and CH_3 deformation	(17, 18)
1523	±20	**Carotenoid**; C=C stretching	(16)
1660	±50	**Cell**; Amide I: C=O stretching, Lipids: C=C stretch vibration	
2160	±50	C≡C stretching	(19)
2920	±50	**Cell**; Lipids/proteins: CH_3 symmetric and antisymmetric stretch, CH_2 antisymmetric stretching	(17)

Table S2. ^{1}H (500 MHz) and ^{13}C (125 MHz) NMR data for protegencin (in DMSO-d_6).

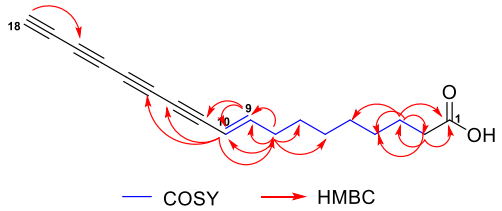

No.	δ_C, type	δ_H, multiplet, J (in Hz)
1	174.4, COOH	11.95, br
2	33.6, CH_2	2.19, t (7.4)
3	24.4, CH_2	1.48, m
4	28.4, CH_2	1.25, m
5	28.4, CH_2	1.25, m
6	28.4, CH_2	1.25, m
7	27.5, CH_2	1.36, m
8	32.8, CH_2	2.19, m
9	154.8, CH	6.65, dt (16.0, 7.1)
10	106.8, CH	5.79, d (16.0)
11	77.4, C	
12	71.8, C	
13	59.7–67.4, C	
14	59.7–67.4, C	
15	59.7–67.4, C	
16	59.7–67.4, C	
17	63.7, C	
18	74.2, CH	4.07, s

377 **Table S3.** Primers for mutation strains of *P. protegens* Pf-5.

Gene	Forward primer	Reverse primer
pgnE Fl1	5'- TGGCTGACGGTCGCAACTCCGG -3'	5'-GCTACTTAATTAAGCTAGCGTAGCCCCTGGATATTGCCGATAAA -3'
pgnE Fl2	5'-GCTACGCTAGCTTAATTAAGTAGCATAACCCGCAGCTGGGAG-3'	5'- GTCGGGCCGGGCCGTTTGACAT -3'
Apr^{R}	5'-GCTACGCTAGCATTCCGGGGATCCGTCGACC-3'	5'-GCTACTTAATTAATGTAGGCTGGAGCTGCTTC-3'

378
379
380

SI Note

While our manuscript was under review, an article reporting an identical polyyne compound (named protegenin A) from *P. protegens* Cab57 was published online May 21, 2021 (received: April 12 2021) (20). In the preceding BioRxiv preprints of our work (B) and of an independent study (A) by Mullins et al. (21), the polyyne from *P. protegens* Pf-5 has been named protegencin.

(A) https://www.biorxiv.org/content/10.1101/2021.03.05.433886v1 (Posted March 6, 2021)

(B) https://www.biorxiv.org/content/10.1101/2021.03.24.436739v1 (Posted March 24, 2021)

Therefore, we decided to keep the name protegencin in the current manuscript.

SI References

1. C. Ross, K. Scherlach, F. Kloss, C. Hertweck, The molecular basis of conjugated polyyne biosynthesis in phytopathogenic bacteria. *Angew. Chem. Int. Ed.* **53**, 7794-7798 (2014).
2. Z. P. Yordanova, E. J. Woltering, V. M. Kapchina-Toteva, E. T. Iakimova, Mastoparan-induced programmed cell death in the unicellular alga *Chlamydomonas reinhardtii*. *AoB Plants* **111**, 191-205 (2012).
3. C. Ding, X. He (2004) K-means clustering via principal component analysis. in *Proceedings of the twenty-first international conference on Machine learning* (Association for Computing Machinery, Banff, Alberta, Canada), p 29.
4. F. Neese, The ORCA program system. *Wiley Interdiscip. Rev. Comput. Mol. Sci.* **2**, 73-78 (2012).
5. F. Neese, Software update: the ORCA program system, version 4.0. *Wiley Interdiscip. Rev. Comput. Mol. Sci.* **8**, e1327 (2018).
6. A. D. Becke, Density-functional thermochemistry. III. The role of exact exchange. *J. Chem. Phys.* **98**, 5648-5652 (1993).
7. C. Lee, W. Yang, R. G. Parr, Development of the Colle-Salvetti correlation-energy formula into a functional of the electron density. *Phys. Rev. B* **37**, 785-789 (1988).
8. F. Weigend, R. Ahlrichs, Balanced basis sets of split valence, triple zeta valence and quadruple zeta valence quality for H to Rn: Design and assessment of accuracy. *Phys. Chem. Chem. Phys.* **7**, 3297-3305 (2005).
9. S. Grimme, J. Antony, S. Ehrlich, H. Krieg, A consistent and accurate ab initio parametrization of density functional dispersion correction (DFT-D) for the 94 elements H-Pu. *J. Chem. Phys.* **132**, 154104 (2010).
10. S. Grimme, S. Ehrlich, L. Goerigk, Effect of the damping function in dispersion corrected density functional theory. *J. Comput. Chem.* **32**, 1456-1465 (2011).
11. K. Eichkorn, O. Treutler, H. Öhm, M. Häser, R. Ahlrichs, Auxiliary basis sets to approximate Coulomb potentials. *Chem. Phys. Lett.* **240**, 283-290 (1995).
12. F. Weigend, Accurate Coulomb-fitting basis sets for H to Rn. *Phys. Chem. Chem. Phys.* **8**, 1057-1065 (2006).
13. P. L. Polavarapu, Ab initio vibrational Raman and Raman optical activity spectra. *J. Phys. Chem.* **94**, 8106-8112 (1990).
14. NIST Computational Chemistry Comparison and Benchmark Database, NIST Standard Reference Database Number 101, Released 20.08.2019, Russell D. Johnson III (Ed.), http://cccbdb.nist.gov/. Accessed 27 October 2020.
15. Y. Ji *et al.*, Raman spectroscopy provides a rapid, non-invasive method for quantitation of starch in live, unicellular microalgae. *Biotechnology Journal* **9**, 1512-1518 (2014).

16. V. E. de Oliveira, H. V. Castro, H. G. Edwards, L. F. C. de Oliveira, Carotenes and carotenoids in natural biological samples: a Raman spectroscopic analysis. *J. Raman Spec.* **41**, 642-650 (2010).
17. C. Krafft, T. Knetschke, R. H. Funk, R. Salzer, Identification of organelles and vesicles in single cells by Raman microspectroscopic mapping. *Vib. Spec.* **38**, 85-93 (2005).
18. J. De Gelder, K. De Gussem, P. Vandenabeele, L. Moens, Reference database of Raman spectra of biological molecules. *J. Raman Spec.* **38**, 1133-1147 (2007).
19. L. Wei *et al.*, Live-cell bioorthogonal chemical imaging: stimulated Raman scattering microscopy of vibrational probes. *Acc. Chem. Res.* **49**, 1494-1502 (2016).
20. K. Murata, M. Suenaga, K. Kai, Genome mining discovery of protegenins A–D, bacterial polyynes involved in the antioomycete and biocontrol activities of *Pseudomonas protegens. ACS Chem. Biol.*, https://doi.org/10.1021/acschembio.1c00276 (2021).
21. Mullins, A. J. *et al.*, Exploration of polyyne biosynthetic gene cluster diversity in bacteria leads to the discovery of the *Pseudomonas* polyyne protegencin. bioRxiv [Preprint] (2021). https://www.biorxiv.org/content/10.1101/2021.03.05.433886v1 (accessed 17 April 2021).